



CHORUS

This is the accepted manuscript made available via CHORUS. The article has been published as:

Shape and symmetry of a fluid-supported elastic sheet

Haim Diamant and Thomas A. Witten

Phys. Rev. E **88**, 012401 — Published 11 July 2013

DOI: [10.1103/PhysRevE.88.012401](https://doi.org/10.1103/PhysRevE.88.012401)

Shape and symmetry of a fluid-supported elastic sheet

Haim Diamant*

*Raymond & Beverly Sackler School of Chemistry,
Tel Aviv University, Tel Aviv 69978, Israel*

Thomas A. Witten†

*Department of Physics and James Franck Institute,
University of Chicago, Chicago, Illinois 60637, USA*

A connection between the dynamics of a sine-Gordon chain and a certain static membrane folding problem was recently found. The one-dimensional membrane profile is a cross-section of the position-time sine-Gordon amplitude profile. Here we show that when one system is embedded in a higher-dimensional system in this way, obvious symmetries in the larger system can lead to nontrivial symmetries in the embedded system. In particular, a thin buckled membrane on a fluid substrate has a continuous degeneracy that interpolates between a symmetric and an antisymmetric fold. We find the Hamiltonian generator of this symmetry and the corresponding conserved momentum by interpreting the simple translational symmetries of the sine-Gordon chain in terms of the embedded coordinates. We discuss possible extensions to other embedded dynamical systems.

PACS numbers: 46.32.+x 46.70.-p 68.60.Bs 81.16.Rf 89.75.Kd

* hdiamant@tau.ac.il

† t-witten@uchicago.edu

I. INTRODUCTION

Thin elastic sheets form rich patterns when stressed or confined. One may try to account for these patterns as weak deformations of a simple (e.g., flat) reference state. It has been recognized, however, that as the sheet is made increasingly thin and bendable, the validity range of such near-threshold analyses shrinks indefinitely, along with their experimental relevance [1–3]. Crumpled paper is a prime example of such a far-from-threshold behavior [4].

A thin elastic sheet, compressed on top of a heavy fluid [5–15], provides a simpler example of this situation. The leading-order analysis of the deformation yields a periodic pattern of wrinkles with wavelength $\lambda = 2\pi[B/(\rho g)]^{1/4}$ [5, 6]. The finite wavelength arises from a competition between the resistance of the sheet to bending (B being the sheet’s bending rigidity) and the resistance of the fluid substrate to height changes (ρ being the fluid mass density and g the gravitational acceleration). Since B depends on the sheet thickness H as $B \sim H^3$, the wrinkling wavelength decreases with decreasing thickness as $\lambda \sim H^{3/4}$. A higher-order analysis reveals that the wrinkling pattern is actually stable only for small lateral displacements, $\Delta < \Delta_w \sim \lambda^2/L$, where L is the total length of the sheet [13, 14]. This validity range diminishes with either decreasing H or increasing L . Beyond it the deformation becomes localized in a finite domain (fold) of width $\kappa^{-1} \sim \lambda^2/\Delta$ [13, 14]. It takes a mere displacement of $\Delta \sim \lambda$ to concentrate all the deformation into a single wavelength and make the fold contact itself [9, 13, 15]. Thus, the relevant response of a sufficiently thin sheet is practically always far from threshold, involving a strong localized deformation. Similar observations hold when the fluid substrate is replaced by an elastic one [14, 16–22].

It is therefore fortunate and beneficial that the fluid-supported sheet under uniaxial compression turns out to be an integrable system [15]. Exactly solvable problems often owe their integrability to extra symmetries. In the current work we focus on the corresponding extra symmetry in the fluid-supported sheet, which is manifest in a continuous degeneracy of ground states [23, 24]. We connect this peculiar property of the one-dimensional buckling problem to the simple translational symmetries of the two-dimensional sine-Gordon problem.

In Secs. II and III we repeat the definition of the problem and its representation as a dynamical system [15]. In Sec. IV we establish the relation between our problem and

the sine-Gordon chain. In Sec. V we characterize the resulting extra symmetry, including consequences concerning the fluid mass displaced by the sheet and the associated buoyant force. Finally, in Sec. VI we discuss consequences of the new symmetry and analogous cases in other physical systems.

II. THE SYSTEM

The system under consideration is schematically illustrated in Fig. 1. An incompressible sheet of bending modulus B lies on a semi-infinite fluid of mass density ρ . The sheet is assumed to be indefinitely long and deform in the xz plane, remaining uncurved along the y axis. The deformation is parameterized by either the height profile $h(u)$ or the slope angular profile $\phi(u)$ as a function of the arclength u along the sheet. The two functions are geometrically linked by the relation $\dot{h} = \sin \phi$, where hereafter a dot denotes a derivative with respect to u . The sheet is subjected at its edges to a uniaxial pressure P along x , which is accompanied by a displacement $\Delta = \int_{-\infty}^{\infty} du(1 - \cos \phi)$ between the two edges.

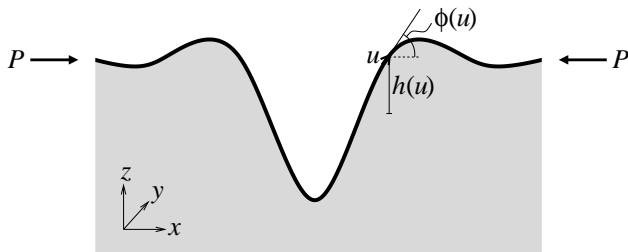


FIG. 1. Schematic view of the system.

A given deformation costs energy per unit length, $E = E_B + E_G$, with contributions from bending, $E_B = (B/2) \int_{-\infty}^{\infty} du \dot{\phi}^2$, and from gravity, $E_G = (K/2) \int_{-\infty}^{\infty} du h^2 \cos \phi$, where $K = \rho g$. We use dimensionless variables, where all lengths are scaled by $(B/K)^{1/4} = \lambda/(2\pi)$ and all energies by B . The pressure is consequently scaled by $(BK)^{1/2}$. An equilibrium shape of the sheet is one that minimizes $E - P\Delta$ for a given P and the appropriate boundary conditions. We thus look for the minimum of the following functional:

$$\begin{aligned} \mathcal{S} &= \int_{-\infty}^{\infty} du \mathcal{L}(\phi, h, \dot{\phi}, \dot{h}) \\ \mathcal{L} &= \frac{1}{2} \dot{\phi}^2 + \frac{1}{2} h^2 \cos \phi - P(1 - \cos \phi) - Q(\sin \phi - \dot{h}). \end{aligned} \quad (1)$$

In Eq. (1) a Lagrange multiplier, $Q(u)$, has replaced the local constraint on the relation between h and ϕ .

III. THE SHEET AS A DYNAMICAL SYSTEM

We study the deformation of the sheet using a mechanical analogy, where the arclength u along the sheet stands for time, and the angle $\phi(u)$ and height $h(u)$ represent two coordinates with conjugate momenta p_ϕ and p_h [15]. The equilibrium shape of the sheet is given by the trajectory $[\phi(u), h(u)]$ that minimizes the action in Eq. (1). The Lagrangian $\mathcal{L}(\phi, h, \dot{\phi}, \dot{h})$ appearing in Eq. (1) transforms into the following Hamiltonian:

$$\mathcal{H}(\phi, h, p_\phi, p_h) = \frac{1}{2}p_\phi^2 + p_h \sin \phi - \frac{1}{2}h^2 \cos \phi + P(1 - \cos \phi). \quad (2)$$

The fact that \mathcal{H} is a constant of motion corresponds to one apparent symmetry of the homogeneous sheet — its invariance to translation in u . In what follows we explicitly distinguish between derivatives with respect to the canonical variables (using the symbol ∂) and derivatives with respect to the coordinates (using dots and primes).

Hamilton's equations yield the following dynamical system:

$$\dot{\phi} = \partial_{p_\phi} \mathcal{H} = p_\phi \quad (3a)$$

$$\dot{h} = \partial_{p_h} \mathcal{H} = \sin \phi \quad (3b)$$

$$\dot{p}_\phi = -\partial_\phi \mathcal{H} = -p_h \cos \phi - (h^2/2 + P) \sin \phi \quad (3c)$$

$$\dot{p}_h = -\partial_h \mathcal{H} = h \cos \phi, \quad (3d)$$

whose solution gives the equilibrium shape. Equations (3a) and (3d) identify the ϕ -conjugate momentum as the local curvature, $p_\phi = \dot{\phi}$, and the h -conjugate momentum as the fluid mass displaced by the deformed sheet up to point u , $p_h = \int_{-\infty}^u du_1 h \cos \phi$. In the case of a localized fold in an infinite sheet the following boundary conditions apply: $h, \phi, \dot{\phi} = p_\phi = 0$ at $u \rightarrow \pm\infty$, resulting in $\mathcal{H} = 0$. Further requiring that $\ddot{\phi} = 0$ far away from the fold implies, through Eq. (3c), that also $p_h = 0$ at $u \rightarrow \pm\infty$. We have found the exact solution of this problem by relating it to the integrable sine-Gordon chain [15]. The integrability of our system implies the existence of a complete set of conserved canonical momenta. Since the system has two canonical momenta, it must thus have two conserved dynamical variables, the Hamiltonian \mathcal{H} and one other. We shall call this conserved quantity \mathcal{K} and determine

it in Sec. V. We need to discuss first the relation between our system and the sine-Gordon chain.

IV. RELATION TO THE SINE-GORDON CHAIN

Equations (3a), (3c), and (2) with $\mathcal{H} = 0$, yield

$$\ddot{\phi} + (\dot{\phi}^2/2 + P)\dot{\phi} + h = 0, \quad (4)$$

which is the known equation of Euler's *elastica* [4, 25], with the hydrostatic pressure term h (ρgh in dimensional terms) playing here the role of an external normal force. Differentiating once with respect to u , we obtain a fourth-order equation for the angle $\phi(u)$ alone,

$$\phi^{(4)} + [(3/2)\dot{\phi}^2 + P]\ddot{\phi} + \sin \phi = 0. \quad (5)$$

Equation (5) is related to a known hierarchy of nonlinear partial differential equations — the combined sine-Gordon and modified KdV (sG-mKdV) hierarchy [26]. The first three equations in that hierarchy, for the two-dimensional function $\phi(u, v)$, read:

$$\dot{\phi}' + 2(\beta e^{i\phi} - \alpha e^{-i\phi}) = 0 \quad (6a)$$

$$\dot{\phi}' - i\ddot{\phi} + 2(\beta e^{i\phi} - \alpha e^{-i\phi}) = 0 \quad (6b)$$

$$\dot{\phi}' + (i/4)\phi^{(4)} + (i/8)\dot{\phi}^2\ddot{\phi} - ic\ddot{\phi} + 2(\beta e^{i\phi} - \alpha e^{-i\phi}) = 0, \quad (6c)$$

where a prime denotes a derivative with respect to v . Note that all equations in the hierarchy are invariant to translations in both coordinates, u and v . Setting $\alpha = \beta = i/4$ in Eq. (6a) yields

$$\dot{\phi}' = \sin \phi. \quad (7)$$

This is the sine-Gordon (SG) equation in light-cone coordinates, $u = (x+t)/2, v = (x-t)/2$, describing the swaying angle $\phi(x, t)$ of a pendulum at position x and time t along a chain of coupled pendulums. Setting in Eq. (6b) $\alpha = \beta = -1/4$ and projecting the equation onto a constant v , we obtain the physical-pendulum (PP) equation,

$$\ddot{\phi} + \sin \phi = 0, \quad (8)$$

where here $\phi(u)$ describes the swaying angle of a single pendulum at time u . Finally, upon setting $\alpha = \beta = 1$ and $c = -P$, and projecting onto a constant v , Eq. (6c) coincides with the shape equation for the sheet, Eq. (5).

The relation to the sG-mKdV hierarchy enables us to obtain solutions of Eq. (5) from known solutions of the PP equation (8) or projected solutions of the SG equation (7). Specifically, we take the “breather” solution of Eq. (7),

$$\phi(u, v) = 4 \tan^{-1} \left[\frac{\kappa \sin(k(u - v + c_1))}{k \cosh(\kappa(u + v + c_2))} \right], \quad k^2 + \kappa^2 = 1, \quad (9)$$

describing a standing localized wave in the chain of pendulums. The two arbitrary constants, c_1 and c_2 , reflect the two symmetries of the SG chain under translations in space x and time t (equivalently, along the two light-cone coordinates u and v). Projection of the breather solution onto one of the light-cone coordinates (e.g., u with $v = 0$) yields the solution to the localized-fold profile,

$$\phi(u) = 4 \tan^{-1} \left[\frac{\kappa \sin(k(u + c_1))}{k \cosh(\kappa(u + c_2))} \right], \quad k^2 + \kappa^2 = 1. \quad (10)$$

Substituting it in Eq. (5), we find

$$k = \frac{1}{2}(2 + P)^{1/2}, \quad \kappa = \frac{1}{2}(2 - P)^{1/2}. \quad (11)$$

The expression for the height profile, $h(u)$, can be obtained in closed form as well but is postponed until the end of Sec. V.

V. THE EXTRA SYMMETRY

The discussion above shows that the folding profiles $\phi(u)$ are embedded in an autonomous two-dimensional system: the sine-Gordon system. The obvious translational invariance of the sine-Gordon system in v entails a corresponding invariance of the folding profiles that is not obvious: not only can the entire profile be translated along the sheet, but the oscillatory and decaying parts of the profile can be shifted independently [cf. Eq. (10)]. Consequently, in between the symmetric fold ($c_1 = c_2 = 0$) and the antisymmetric one ($c_1 k = \pi/2$, $c_2 = 0$) there exists a continuous family of degenerate profiles, having the exact same displacement and the exact same (minimum) energy [23, 24]. This is demonstrated in Fig. 2.

We can directly demonstrate that the specific solution presented in the preceding section satisfies this symmetry—i.e., that shifting v in the profile of Eq. (9) leaves all energy terms invariant. The purpose of the current section, however, is to establish and characterize the extra symmetry at the level of the original functional to be minimized, Eq. (1). Thus, any other solution to the problem will have to satisfy this symmetry as well.

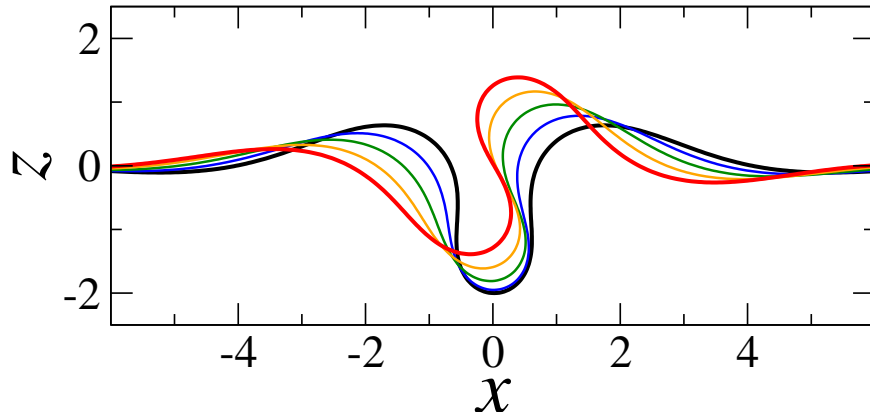


FIG. 2. (color online). Shapes of a folded sheet for $P = 1$. In between the symmetric fold (lowest black curve) and the antisymmetric one (uppermost red curve) there is a continuum of degenerate shapes having the exact same displacement and energy. The shapes were calculated from Eqs. (10) and (11) with $c_2 = 0$ and $c_1 k = 0, \pi/8, \pi/4, 3\pi/8$, and $\pi/2$.

A. Conservation law

To find the conserved quantity associated with the extra symmetry, $\mathcal{K}(\phi, h, p_\phi, p_h)$, we seek the generator of v -translations in the Hamiltonian phase space of Eq. (2),

$$\{f, \mathcal{K}\} = f', \quad (12)$$

where $f(u, v)$ is an arbitrary function expressed in terms of our canonical variables [Eq. (2)], and $\{\dots\}$ are Poisson brackets. In the derivation below we make use of the following: (a) our knowledge of the first conserved quantity, \mathcal{H} [Eq. (2)], and the resulting Hamilton equations (3); (b) the set of equations, analogous to Hamilton's, that derive from \mathcal{K} , i.e., $\{\phi, \mathcal{K}\} = \partial_{p_\phi} \mathcal{K}$, $\{h, \mathcal{K}\} = \partial_{p_h} \mathcal{K}$, $\{p_\phi, \mathcal{K}\} = -\partial_\phi \mathcal{K}$, $\{p_h, \mathcal{K}\} = -\partial_h \mathcal{K}$; (c) the fact that $\phi(u, v)$ should satisfy the SG equation (7). (Note, however, that we make no use of any particular solution of the SG equation.) Below we obtain a set of differential constraints on \mathcal{K} , find a functional form consistent with these, and finally verify that this \mathcal{K} , (a) generates the desired shift in v , and (b) commutes with \mathcal{H} .

Taking $f = \phi$ in Eq. (12) and differentiating both sides with respect to u , we find $(d/du)\{\phi, \mathcal{K}\} = \dot{\phi}' = \sin \phi = \dot{h}$. Thus, up to an integration constant, taken as zero,

$$\partial_{p_\phi} \mathcal{K} = \phi' = h. \quad (13)$$

We note that the equation $\phi' = h$ provides the connection between the coordinate v and the actual sheet,

$$hdv = \dot{\phi} du.$$

It also represents the fact (now in terms of v rather than u) that ϕ and h are inter-independent; just as $\dot{h} = \sin \phi$ along the u coordinate, $\phi' = h$ along the v coordinate. Applying a similar procedure with $f = h$ yields $(d/du)\{h, \mathcal{K}\} = \dot{h}' = (\sin \phi)' = \cos \phi \phi' = h \cos \phi = \dot{p}_h$. Thus, up to an integration constant,

$$\partial_{p_h} \mathcal{K} = p_h. \quad (14)$$

Next, for $f = p_\phi$, we have $\{p_\phi, \mathcal{K}\} = p'_\phi = \dot{\phi}' = \sin \phi$. Thus,

$$\partial_\phi \mathcal{K} = -\sin \phi. \quad (15)$$

Finally, for $f = p_h$, we get $(d/du)\{p_h, \mathcal{K}\} = \dot{p}'_h = (h \cos \phi)' = \cos \phi h' - h \sin \phi \phi' = p_h \cos \phi - h^2 \sin \phi$. Using Hamilton's equation (3c), we write this result as $(d/du)\{p_h, \mathcal{K}\} = -\dot{p}_\phi - [(3/2)h^2 + P] \sin \phi = -(d/du)[p_\phi + h^3/2 + Ph]$. Thus, up to an integration constant,

$$\partial_h \mathcal{K} = p_\phi + \frac{1}{2}h^3 + Ph. \quad (16)$$

Gathering the information from Eqs. (13)–(16), we obtain an expression for the second conserved quantity,

$$\mathcal{K} = \frac{1}{2}p_h^2 + hp_\phi + \frac{1}{2}h^2(h^2/4 + P) - (1 - \cos \phi). \quad (17)$$

We may now verify that this candidate form for \mathcal{K} satisfies the requirements (a) and (b) above. By construction, the \mathcal{K} of Eq. (17) satisfies Eqs. (13)–(16). Thus, it generates a shift in v , fulfilling requirement (a). To address requirement (b) we may explicitly verify that \mathcal{K} of Eq. (17) is a constant of motion,

$$\{\mathcal{K}, \mathcal{H}\} = (\partial_\phi \mathcal{K})(\partial_{p_\phi} \mathcal{H}) - (\partial_{p_\phi} \mathcal{K})(\partial_\phi \mathcal{H}) + (\partial_h \mathcal{K})(\partial_{p_h} \mathcal{H}) - (\partial_{p_h} \mathcal{K})(\partial_h \mathcal{H}) = 0, \quad (18)$$

as can be verified by direct substitution using Eqs. (13)–(16). While this \mathcal{K} bears no obvious resemblance to \mathcal{H} of Eq. (2), the two must nevertheless be equivalent in generating the fold. The SG equation (7) is invariant to interchanging u and v , and a localized SG solution along

a line of constant u must be equivalent to that along a line of constant v . To verify this duality we form the Hamilton equations generated by \mathcal{K} ,

$$\phi' = \partial_{p_\phi} \mathcal{K} = h \quad (19a)$$

$$h' = \partial_{p_h} \mathcal{K} = p_h \quad (19b)$$

$$p'_\phi = -\partial_\phi \mathcal{K} = \sin \phi \quad (19c)$$

$$p'_h = -\partial_h \mathcal{K} = -p_\phi - h^3/2 - Ph. \quad (19d)$$

When the two dynamical systems (3) and (19) are compared, their equivalence is not obvious. The replacement $h \leftrightarrow p_\phi$, however, makes Eqs. (19a) and (19c) the same as Eqs. (3a) and (3b), respectively, and Eqs. (19b) and (19d) yield Eq. (4) of Euler's *elastica*. Once a single equation for $\phi(v)$ is constructed,

$$\phi'''' + [(3/2)(\phi')^2 + P]\phi'' + \sin \phi = 0, \quad (20)$$

and compared with Eq. (5), the equivalence is apparent.

Finally, we use the extra symmetry to obtain closed-form expressions which could not be derived in earlier works. The height profile, $h(u) = \int_{-\infty}^u du_1 \sin \phi$, is obtained according to Eq. (19a) by differentiating the breather, Eq. (9), with respect to v and then setting $v = 0$. We get

$$h(u) = -4k\kappa \frac{k \cos \tilde{u}_1 \cosh \tilde{u}_2 + \kappa \sin \tilde{u}_1 \sinh \tilde{u}_2}{k^2 \cosh^2 \tilde{u}_2 + \kappa^2 \sin^2 \tilde{u}_1} \quad (21)$$

$$\tilde{u}_1 = k(u + c_1), \quad \tilde{u}_2 = \kappa(u + c_2).$$

Similarly, according to Eq. (19b), we obtain the profile of displaced fluid mass, $p_h = \int_{-\infty}^u du_1 h \cos \phi$, by differentiating the breather twice with respect to v and setting $v = 0$. This yields

$$p_h(u) = \frac{2k\kappa}{(k^2 \cosh^2 \tilde{u}_2 + \kappa^2 \sin^2 \tilde{u}_1)^2} [2k\kappa\{k^2 \cosh(2\tilde{u}_2) + \kappa^2 \cos(2\tilde{u}_1) + k^2 - \kappa^2\} \cos \tilde{u}_1 \sinh \tilde{u}_2 - \{(k^2 - \kappa^2)[k^2 \cosh(2\tilde{u}_2) + \kappa^2 \cos(2\tilde{u}_1)] + k^4 + 6k^2\kappa^2 + \kappa^4\} \sin \tilde{u}_1 \cosh \tilde{u}_2]. \quad (22)$$

B. Shape transformation

The actual transformation generated by the extra symmetry is nontrivial. From Eqs. (19a) and (19b) we see that a slight translation δv in the extra dimension adds to the

angle of the sheet at each point a small amount proportional to the height at that point, $\phi(u) \rightarrow \phi(u) + h(u)\delta v$; to the height it adds a small amount proportional to p_h , the fluid mass displaced up to that point, $h(u) \rightarrow h(u) + p_h(u)\delta v$. In Fig. 2 one can try to follow these small changes between consecutive curves.

We verify that such an infinitesimal transformation leaves the mechanical energy of the sheet unchanged. Applying it to the bending energy, we get

$$\frac{\delta E_B}{\delta v} = \dot{\phi}\dot{h} = \sin\phi\dot{\phi} = -(d/du)(\cos\phi), \quad (23)$$

which is a total differential, contributing only a boundary term to the integrated bending energy. That contribution vanishes for our boundary conditions. For the gravitational energy we get, with the help of Eq. (3d),

$$\frac{\delta E_G}{\delta v} = hp_h \cos\phi - \frac{1}{2}h^3 \sin\phi = p_h\dot{p}_h - \frac{1}{2}h^3\dot{h} = (d/du)(p_h^2/2 - h^4/8), \quad (24)$$

which is a total differential as well. The contribution from the h^4 term vanishes for our boundary conditions; the vanishing of the second boundary contribution is discussed in the next subsection. Thus, both the bending energy and the substrate energy are *separately* invariant to the transformation. We further confirm that the functional giving the displacement for a given P is invariant too,

$$\frac{\delta\Delta}{\delta v} = h \sin\phi = h\dot{h} = (d/du)(h^2/2). \quad (25)$$

Finally, the variations $\delta\dot{h}/\delta v = \dot{p}_h$ and $\delta \sin\phi/\delta v = h \cos\phi$ are equal thanks to Eq. (3d), ensuring that the transformation does not violate the geometrical constraint $\dot{h} = \sin\phi$.

C. Buoyant force

When defining the system in Sec. II, we have prescribed the lateral force per unit length acting on the sheet, P , which is coupled to the lateral displacement, Δ . By contrast, no explicit term has been introduced to impose an external vertical force or a certain vertical displacement, apart from the boundary condition $h(u \rightarrow \pm\infty) = 0$. This is equivalent to imposing a zero vertical force. In the absence of such an external force, the total vertically displaced fluid mass must vanish. The localized solutions of the profile equation should automatically satisfy this constraint.

As mentioned above, the mass of vertically displaced fluid up to a certain point u in the sheet is equal to the h -conjugate momentum, $p_h = \int_{-\infty}^u du_1 h \cos \phi$ [cf. Eq. (3d)]. Thus, the total displaced fluid mass is $M_f = p_h(\infty)$. The fact that $M_f = 0$ then readily follows from Eq. (3c) applied at $u \rightarrow \infty$. It is inferred also from the conservation of \mathcal{K} when setting $\mathcal{K}(-\infty) = \mathcal{K}(\infty)$ in Eq. (17). Finally, we explicitly confirm that $p_h(\pm\infty) \rightarrow 0$ using the closed-form expression for p_h , Eq. (22).

VI. DISCUSSION

The physical property of the sheet–fluid composite, underlying the extra symmetry, is unclear. We have found no physical argument to explain why the shape transformation described in Sec. V B leaves the mechanical energy of the sheet invariant. Nonetheless, in the two-dimensional problem, in which we have embedded our one-dimensional system, the extra symmetry is a trivial translation invariance along the extra dimension. The surprising fact that the different energy contributions are *individually* invariant to the shape transformation generated by \mathcal{K} follows as well from an evident symmetry of the sine-Gordon chain—the invariance to exchange of its two light-cone coordinates (which in turn derives from the time-reversal symmetry of the chain of pendulums). Each energy term is obviously invariant to translation along the sheet (i.e., translation in u) and, therefore, due to the $u \leftrightarrow v$ symmetry, must be individually invariant also to translation in v .

This situation is reminiscent of the phason freedom in quasicrystals [27–29]. In the actual quasicrystal the degenerate phason states correspond to nontrivial coordinated flips of atom locations. Yet, once the quasicrystal is represented as a projection of a higher-dimensional Bravais lattice [28], the phason flips are obtained from simple lattice translations along the extra dimensions. An important distinction between the new symmetry and phasons is that the generated transformation is continuous rather than discrete. Thus, there are no energy barriers between the degenerate shapes. Boundary conditions are expected to remove the degeneracy and will usually favor the symmetric and/or antisymmetric states [9]. The corresponding energy differences, however, should be exponentially small in κL . Therefore, we anticipate important consequences of the continuous degeneracy for the dynamics of ultra-thin fluid-supported films.

On the face of it, the \mathcal{K} symmetry arises only from the *translational* invariance of the two-

dimensional host system in which it is embedded. There is no apparent need for *integrability* of the host system. Yet, when one attempts to determine \mathcal{K} in practice for a non-integrable host system, the procedure of Eqs. (12)–(16) fails. The differential conditions imposed by these equations do not integrate to a well-defined function of (ϕ, h, p_ϕ, p_h) . The requirement that these conditions must define a definite \mathcal{K} function may then be a way of formulating the condition for integrability of the host system.

The floating elastic sheets discussed here occur widely in physical systems, especially in molecular and nanoparticle monolayers [9, 10, 30]. Thus we expect the degenerate shapes described above to have physical implications. First, one should in principle see the degeneracy in the model experiments on macroscopic sheets where this folding was initially demonstrated [9]. However, only the symmetric and antisymmetric folds were reported. These sheets had lengths L not much greater than the width of the deformed region, so that boundary effects not considered here could have broken the degeneracy. In molecular sheets [31] one may imagine a distortion of the y -invariant fold in which the asymmetry parameter varies slowly along the y direction, as demonstrated in Fig. 3. The extra energy for such a distortion must vanish as its wavelength goes to infinity, even though its amplitude is large. Here too, extra effects may act to select one or another of the asymmetric folds. For example, self-attraction favors the symmetric fold, since this variant approaches itself more closely than the others. On the other hand, the formation of a fold requires viscous dissipation, enhanced by shear stress. This stress is likely greater in the symmetric fold, so that the antisymmetric fold should be kinetically favored.

The symmetry and degeneracy found here were an indirect and mysterious consequence of the integrability of the two-dimensional host system. Though we have discussed it in the context of a particular embedded system of physical interest, we expect that analogous symmetries occur elsewhere in the sG-mKdV hierarchy. These symmetries may ultimately deepen our understanding of integrability in these systems. In physical terms these degenerate deformations and the aforementioned “soft modes” associated with them may ultimately shed light on the experimental puzzles of how molecular folding and unfolding occur in practice [30–32].

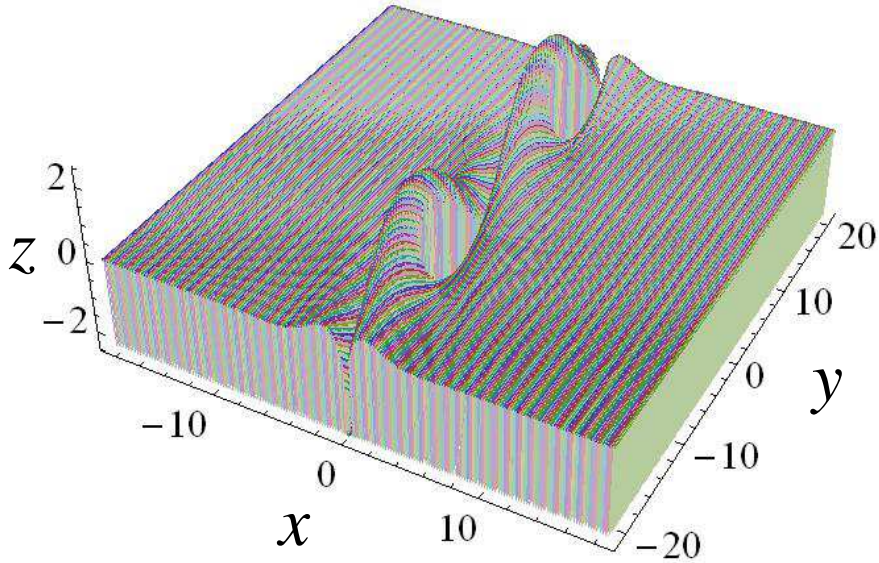


FIG. 3. (color online). Shape of a folded sheet whose y -invariance is broken by a “soft v -mode”. Each xz cut is one of the degenerate solutions given by Eq. (10) with $c_2 = 0$ and c_1 that changes linearly with y . The pressure is $P = 0.5$.

ACKNOWLEDGMENTS

We thank Ron Lifshitz for a helpful discussion. This work was supported in part by the University of Chicago MRSEC program of the NSF under Award Number DMR 0820054.

-
- [1] B. Davidovitch, R. D. Schroll, D. Vella, M. Adda-Bedia, and E. A. Cerda, Proc. Natl. Acad. Sci. USA **108**, 18227 (2011).
 - [2] B. Davidovitch, R. D. Schroll, and E. Cerda, Phys. Rev. E **85**, 066115 (2012).
 - [3] H. King, R. D. Schroll, B. Davidovitch, and N. Menon, Proc. Natl. Acad. Sci. USA **109**, 9716 (2012).
 - [4] T. A. Witten, Rev. Mod. Phys. **79**, 643 (2007).
 - [5] S. T. Milner, J.-F. Joanny, and P. Pincus, Europhys. Lett. **9**, 495 (1989).
 - [6] E. Cerda and L. Mahadevan, Phys. Rev. Lett. **90**, 074302 (2003).
 - [7] D. Vella, P. Aussillous, and L. Mahadevan, Europhys. Lett. **68**, 212 (2004).

- [8] J. Huang, M. Juskiewicz, W. H. de Jeu, E. Cerda, T. Emrick, N. Menon, and T. P. Russell, *Science* **317**, 650 (2007).
- [9] L. Pocivavsek, R. Dellsy, A. Kern, S. Johnson, B. Lin, K. Y. C. Lee, and E. Cerda, *Science* **320**, 912 (2008).
- [10] B. D. Leahy, L. Pocivavsek, M. Meron, K. L. Lam, D. Salas, P. J. Viccaro, K. Y. C. Lee, and B. Lin, *Phys. Rev. Lett.* **105**, 058301 (2010).
- [11] J. Huang, B. Davidovitch, C. D. Santangelo, T. P. Russell, and N. Menon, *Phys. Rev. Lett.* **105**, 038302 (2010).
- [12] D. P. Holmes and A. J. Crosby, *Phys. Rev. Lett.* **105**, 038303 (2010).
- [13] H. Diamant and T. A. Witten, arXiv:1009.2487.
- [14] B. Audoly, *Phys. Rev. E* **84**, 011605 (2011).
- [15] H. Diamant and T. A. Witten, *Phys. Rev. Lett.* **107**, 164302 (2011).
- [16] J. M. T. Thompson and G. W. Hunt, *A General Theory of Elastic Stability* (Wiley, London, 1973).
- [17] G. W. Hunt, M. K. Wadee, and N. Shiacolas, *J. Appl. Mech.* **60**, 1033 (1993).
- [18] S. H. Lee and A. M. Waas, *Int. J. Non-Linear Mech.* **31**, 313 (1996).
- [19] Q. Zhang and T. A. Witten, *Phys. Rev. E* **76**, 041608 (2007).
- [20] B. Audoly and A. Boudaoud, *J. Mech. Phys. Solids* **56**, 2401 (2008).
- [21] P. M. Reis, F. Corson, A. Boudaoud, and B. Roman, *Phys. Rev. Lett.* **103**, 045501 (2009).
- [22] F. Brau, H. Vandeparre, A. Sabbah, C. Poulard, A. Boudaoud, and P. Damman, *Nat. Phys.* **7**, 56 (2011).
- [23] H. Diamant and T. A. Witten, Talk presented at the APS Meeting, Boston, March 2012, <http://meetings.aps.org/link/BAPS.2012.MAR.L52.10>
- [24] M. Rivetti, *C. R. Mec.* **341**, 333 (2013).
- [25] E. Cerda and L. Mahadevan, *Proc. R. Soc. A* **461**, 671 (2005).
- [26] F. Gesztesy and H. Holden, *Soliton Equations and Their Algebro-Geometric Solutions* (Cambridge University Press, Cambridge, 2003), Chapter 2.
- [27] D. Levine, T. C. Lubensky, S. Ostlund, S. Ramaswamy, P. J. Steinhardt, and J. Toner, *Phys. Rev. Lett.* **54**, 1520 (1985).
- [28] P. A. Kalugin, A. Yu. Kitaev, and L. S. Levitov, *JETP Lett.* **41**, 145 (1985).
- [29] R. Lifshitz, *Isr. J. Chem.* **51**, 1156 (2011).

- [30] K. Y. C. Lee, *Ann. Rev. Phys. Chem.* **59**, 771 (2008).
- [31] Y. Zhang and T. M. Fischer, *J. Phys. Chem. B* **109**, 3442 (2005).
- [32] A. Gopal, V. Belyi, H. Diamant, T. A. Witten, K. Y. C. Lee, *J. Phys. Chem. B* **110**, 10220 (2006).